

# Fit to Moments of Inclusive $B \rightarrow X_c \ell \bar{\nu}$ and $B \rightarrow X_s \gamma$ Decay Distributions using Heavy Quark Expansions in the Kinetic Scheme

O. L. Buchmüller  
CERN, CH-1211 Geneva 23, Switzerland

H. U. Flächer  
Royal Holloway, University of London, Egham, Surrey TW20 0EX, United Kingdom  
(Dated: December 29, 2005)

We present a fit to measured moments of inclusive distributions in  $B \rightarrow X_c \ell \bar{\nu}$  and  $B \rightarrow X_s \gamma$  decays to extract values for the CKM matrix element  $|V_{cb}|$ , the b- and c-quark masses, and higher order parameters that appear in the Heavy Quark Expansion. The fit is carried out using theoretical calculations in the kinetic scheme and includes moment measurements of the *BABAR*, *Belle*, *CDF*, *CLEO* and *DELPHI* collaborations for which correlation matrices have been published. We find  $|V_{cb}| = (41.96 \pm 0.23_{\text{exp}} \pm 0.35_{\text{HQE}} \pm 0.59_{\Gamma_{SL}}) \times 10^{-3}$  and  $m_b = 4.590 \pm 0.025_{\text{exp}} \pm 0.030_{\text{HQE}} \text{ GeV}$  where the errors include experimental and theoretical uncertainties. We also derive values for the heavy quark distribution function parameters  $m_b$  and  $\mu_\pi^2$  in different theoretical schemes that can be used as input for the determination of  $|V_{ub}|$ .

PACS numbers: 12.15.Ff, 12.15.Hh, 12.39.Hg, 13.30.Ce

## I. INTRODUCTION

In the past few years tremendous progress has been made in the description of semileptonic and radiative  $B$  decays using the framework of Heavy Quark Expansions (HQEs). Calculations for the semileptonic decay width as well as for moments of inclusive observables with restrictions on the phase space are now available in different schemes through order  $1/m_b^3$  and  $\alpha_s^2 \beta_0$  [1, 2, 3, 4, 5, 6]. At the same time many new experimental measurements of moments of the hadronic mass and lepton energy distribution in  $B \rightarrow X_c \ell \bar{\nu}$  as well as the photon energy spectrum in  $B \rightarrow X_s \gamma$  decays have been carried out by several experiments. Generally, the results agree very well between experiments. In addition, the theoretical calculations describe the measured data well establishing this framework for treating semileptonic and radiative  $B$  decays [7, 8, 9].

In this document we will present the results of a combined fit to measured moments for which correlation matrices are published. These include moments of the hadronic mass distribution  $\langle M_X^n \rangle$  and moments of the lepton energy spectrum  $\langle E_\ell^n \rangle$  in inclusive  $B \rightarrow X_c \ell \bar{\nu}$  decays as well as moments of the photon energy spectrum  $\langle E_\gamma^n \rangle$  in inclusive  $B \rightarrow X_s \gamma$  decays for different minimum lepton and photon energies  $E_{\text{cut}}$ . The HQEs for the moments depend on the b- and c- quark masses and several non-perturbative parameters which therefore can be determined from a fit of the theoretical expressions to the experimental moment measurements. Among the measurements we have excluded those for which there are ongoing discussions within the theoretical community regarding the associated theoretical uncertainties. These are in particular the non-integer moments  $\langle M_X \rangle$  and  $\langle M_X^3 \rangle$  of the hadronic mass distribution in  $B \rightarrow X_c \ell \bar{\nu}$  decays. In addition, moments of the photon energy spec-

trum in  $B \rightarrow X_s \gamma$  decays above  $E_{\text{cut}} = 2.0 \text{ GeV}$  have been excluded since there the standard local Operator Product Expansion (OPE) is no longer believed to be under theoretical control. Furthermore, individual moment measurements have been discarded if the covariance matrix cannot be inverted due to the large correlations between the measurements.

## II. HEAVY QUARK EXPANSIONS IN THE KINETIC SCHEME

In this analysis we make use of HQEs that express the semileptonic decay width  $\Gamma_{SL}$  as well as moments of the lepton energy and hadron mass distribution in  $B \rightarrow X_c \ell \bar{\nu}$  decays and those of the photon energy spectrum in  $B \rightarrow X_s \gamma$  decays in terms of the running kinetic quark masses  $m_b(\mu)$  and  $m_c(\mu)$ . Non-perturbative effects are introduced in this formalism via heavy quark operators. The leading power corrections arise at  $O(1/m_b^2)$  and are controlled by the two expectation values  $\mu_\pi^2(\mu)$  and  $\mu_G^2(\mu)$  of the kinetic and chromomagnetic dimension-five operators. At  $O(1/m_b^3)$  two additional expectation values  $\rho_D^3(\mu)$  and  $\rho_{LS}^3(\mu)$  of the Darwin and spin-orbital (LS) dimension-six operators complete the set of non-perturbative corrections. Together with the two running quark masses the HQE in the kinetic scheme includes six free parameter through  $O(1/m_b^3)$ :

- Leading Order Parameters
  - $m_b(\mu) \rightarrow$  b-quark mass
  - $m_c(\mu) \rightarrow$  c-quark mass
- Leading Non-Perturbative Corrections -  $O(1/m_b^2)$ 
  - $\mu_\pi^2(\mu) \rightarrow$  ‘kinetic expectation value’
  - $\mu_G^2(\mu) \rightarrow$  ‘chromomagnetic expectation value’

- Higher Order Non-Perturbative Corrections -  $O(1/m_b^3)$ 
  - $\rho_D^3(\mu)$  → ‘Darwin term’
  - $\rho_{LS}^3(\mu)$  → ‘spin-orbital term’

At any given value of the Wilsonian factorization scale  $\mu$  all of the above mentioned HQE parameters represent well defined physical quantities which have to be determined from measurements. The scale  $\mu$  separates ‘short-distance’ effects from ‘long-distance’ effects and, therefore,  $m_Q(\mu)$  can be understood as a short-distance mass of perturbation theory that excludes soft gluon interactions [3]. It is important to note that Ref. [3] contains a translation to full order  $\alpha_s^2$  and third-order BLM corrections of the running short-distance mass  $m_Q(\mu)$  into the well known running  $\overline{\text{MS}}$  mass  $\overline{m}_Q(\overline{m}_Q)$ . Hence the kinetic masses  $m_b(\mu)$  and  $m_c(\mu)$  can be compared with other established mass definitions in QCD such as the  $\overline{\text{MS}}$  mass. This fact is important for the comparison with other QCD calculations beyond semileptonic or rare B-decays. In order to minimize the influence of radiative corrections and to insure that the kinetic c-quark mass  $m_c(\mu)$  has a well defined physical meaning the separation scale is set to be  $\mu = 1$  GeV. A detailed discussion of the justification for this choice can be found in Ref. [10]. In the following, all heavy quark parameter values are presented for  $\mu = 1$  GeV (e.g.  $m_b(1$  GeV) →  $m_b$ ). The analytical expression for the semileptonic width of  $B \rightarrow X_c \ell \bar{\nu}$  decays through  $O(1/m_b^3)$  [3] is given by

$$\Gamma_{SL}(B \rightarrow X_c \ell \bar{\nu}) = \frac{G_F^2 m_b^5}{192\pi^3} |V_{cb}|^2 (1 + A_{ew}) A_{pert}(r, \mu) \times \left[ z_0(r) \left( 1 - \frac{\mu_\pi^2 - \mu_G^2 + \frac{\rho_D^3 + \rho_{LS}^3}{m_b}}{2m_b^2} \right) - 2(1-r)^4 \frac{\mu_G^2 + \frac{\rho_D^3 + \rho_{LS}^3}{m_b}}{m_b^2} + d(r) \frac{\rho_D^3}{m_b^3} + O(1/m_b^4) \right], \quad (1)$$

where  $r = m_c^2/m_b^2$  explicitly contains the c-quark mass  $m_c$ . The tree level phase space factor  $z_0$  is defined through:

$$z_0(r) = 1 - 8r + 8r^3 - r^4 - 12r^2 \ln(r) ,$$

and the expression  $d(r)$  is given by:

$$d(r) = 8 \ln(r) + \frac{34}{3} - \frac{32}{3}r - 8r^2 + \frac{32}{3}r^3 - \frac{10}{3}r^4 .$$

The electroweak corrections for Eq. 1 are estimated to be approximately

$$1 + A_{ew} \approx \left( 1 + \frac{\alpha}{\pi} \ln \frac{M_Z}{m_b} \right)^2 \approx 1.014 ,$$

and the perturbative contributions, which have been calculated to all orders in BLM corrections and to second order in non-BLM corrections, are for a reasonable set

of HQE parameters estimated to be  $A_{pert} \approx 0.908$ . It should be noted that Eq. 1 is not a HQE in powers of  $1/m_b$ . Since the most relevant scale for the  $b \rightarrow c$  transition is the energy release  $m_b - m_c$  of the decay rather than the b-quark mass  $m_b$ , this expansion is carried out in powers of  $1/(m_b - m_c)$ . On the other hand, due to the low mass of the  $s$ - and  $u$ -quark, HQE calculations for the  $b \rightarrow s$  or  $b \rightarrow u$  transition can be considered as expansions in powers of  $1/m_b$ . The full  $\alpha_s^2$  corrections to the photon spectrum have been computed recently [11]. As follows from this result, the effects of omitting the non-BLM corrections are small and fully covered by the assumed theoretical uncertainties we quote for the first and second photon energy moments.

For the practical use Eq. 1 can be transformed into:

$$\begin{aligned} \frac{|V_{cb}|}{|V_{cb}^0|} = & \left( \frac{BR_{c\ell\bar{\nu}}}{0.105 - 0.0018} \right)^{\frac{1}{2}} \left( \frac{1.55\text{ps}}{\tau_B} \right)^{\frac{1}{2}} (1 \pm \delta_{th}) \\ & \times [1 + 0.30 (\alpha_s(m_b) - 0.22)] \\ & \times [1 - 0.66 (m_b - 4.6 \text{ GeV}) + 0.39 (m_c - 1.15 \text{ GeV}) \\ & + 0.013 (\mu_\pi^2 - 0.4 \text{ GeV}^2) + 0.09 (\tilde{\rho}_D^3 - 0.1 \text{ GeV}^3) \\ & + 0.05 (\mu_G^2 - 0.35 \text{ GeV}^2) - 0.01 (\rho_{LS}^3 + 0.15 \text{ GeV}^3)] , \end{aligned} \quad (2)$$

where  $|V_{cb}^0| = 0.0417$  and  $\tau_B$  represents the average lifetime of neutral and charged B mesons. We use  $\tau_B = 1.585 \pm 0.007$  ps based on Ref. [12], assuming equal production of charged and neutral B mesons. The theoretical uncertainty due to the limited accuracy of this HQE is denoted by  $\delta_{th}$ . In Ref. [3] its value is quoted with  $\delta_{th} = 0.015$ , with contributions from four different sources. Since then a more elaborate study on the influence of ‘intrinsic charm’ has been carried out reducing the associated uncertainty by roughly a factor two [13], leaving an overall uncertainty of  $\delta_{th} = 0.014$ . More details about this theoretical uncertainty can be found in Section III C. It should be noted that we do not extract the Darwin term  $\rho_D^3(1$  GeV) directly from our fit to the HQEs but rather the ‘pole-type’ Darwin expectation value  $\tilde{\rho}_D^3$ . The two parameters are closely related in our framework via

$$\tilde{\rho}_D^3 = \rho_D^3(1 \text{ GeV}) - 0.1 \text{ GeV}^3 .$$

Relations similar to Eq. 2 have been calculated for inclusive observables in semileptonic and radiative B decays. These are in particular hadron mass  $\langle M_X^n \rangle$  and lepton energy moments  $\langle E_\ell^n \rangle$  to order  $n$  as well as moments of the photon energy spectrum  $\langle E_\gamma^n \rangle$ :

$$\begin{aligned} \langle M_X^n \rangle & \rightarrow \langle M_X \rangle (m_b, m_c, \mu_\pi^2, \mu_G^2, \rho_D^3, \rho_{LS}^3, \alpha_s) \\ \langle E_\ell^n \rangle & \rightarrow \langle E_\ell^n \rangle (m_b, m_c, \mu_\pi^2, \mu_G^2, \rho_D^3, \rho_{LS}^3, \alpha_s) \\ \langle E_\gamma^n \rangle & \rightarrow \langle E_\gamma^n \rangle (m_b, \mu_\pi^2, \mu_G^2, \rho_D^3, \rho_{LS}^3, \alpha_s) . \end{aligned}$$

Since every moment calculation has a different dependence on the heavy quark parameters a simultaneous fit allows for the extraction of all these parameters. For this it is important to use as many moment measurements as possible in order to overconstrain the extraction of the heavy quark parameters and to establish the validity of the expansions. A much more detailed description of the theoretical framework used for this analysis can be found in Refs. [2, 3, 4].

### III. FIT TO MOMENT MEASUREMENTS

In the following sections we list the currently available experimental moment measurements and indicate which are used in the combined fit presented here. Furthermore, we outline the fit procedure and summarize the results obtained from two different fit scenarios and various cross checks.

#### A. Experimental Input

All results are based on the following set of moment measurements which are also summarised in Table I. Additional measurements for which correlation matrices are not available and thus cannot be used in the presented fit are listed in parentheses.

- **BABAR**

Hadron mass [14] and lepton energy moments [15] from  $B \rightarrow X_c \ell \bar{\nu}$  decays measured as a function of the minimum lepton energy  $E_{\text{cut}}$ . The lepton moments used here differ slightly from those in the *BABAR* publication [15]. They have been updated by taking into account the recent improved measurements of the  $D_s$  and  $B$  branching fractions (*upper-vertex charm*) that impact the background subtraction. Moments of the photon energy spectrum in  $B \rightarrow X_s \gamma$  decays as a function of the minimum photon energy  $E_{\text{cut}}$  from two independent analyses [16, 17].

- **Belle**

First and second moment of the photon energy spectrum as a function of the minimum photon energy  $E_{\text{cut}}$  [18, 19].

(Measurements of hadron mass and lepton energy moments as functions of the lower lepton energy exist [20, 21] but are excluded from the current fit as correlation matrices are only available for the statistical errors.)

- **CDF**

Hadron moment measurements with a minimum lepton energy of  $E_{\text{cut}} = 0.7$  GeV [22].

- **CLEO**

Hadron moment measurements as a function of the minimum lepton energy [23].

First (and second) moment of the photon energy spectrum at  $E_{\text{cut}} = 2.0$  GeV [24].

(The measurement of lepton energy moments as a function of  $E_{\text{cut}}$  [25] is not given with the full covariance matrix and thus has not been included in the fit [26].)

- **DELPHI**

Lepton energy and hadron mass moment measurements with no restriction on the lepton energy [27].

#### B. Fit Procedure

A  $\chi^2$  minimization technique is used to determine the HQE predictions in the kinetic scheme from a fit to the data:

$$\chi^2 = (\vec{M}_{\text{exp}} - \vec{M}_{\text{HQE}})^T C_{\text{tot}}^{-1} (\vec{M}_{\text{exp}} - \vec{M}_{\text{HQE}}) \quad (3)$$

where  $\vec{M}_{\text{exp}}$  represents all moment measurements included in the fit and  $\vec{M}_{\text{HQE}}$  stands for their HQE prediction defined by the heavy quark parameters.  $C_{\text{tot}} = C_{\text{exp}} + C_{\text{theo}}$  is the sum of the experimental and theoretical covariance matrices. The construction of the theoretical covariance matrix  $C_{\text{theo}}$  is discussed in detail in Section III C.

In order to extract the semileptonic branching fraction for  $B \rightarrow X_c \ell \bar{\nu}$  events  $BR_{c\ell\bar{\nu}}$  from the fit, the measurements of the truncated branching fractions  $\langle E_L^0 \rangle$  at different cutoffs in the lepton energy  $E_{\text{cut}}$  are also used as experimental input. HQE predictions of the relative decay fraction for a given cutoff  $E_{\text{cut}}$ ,

$$R(E_{\text{cut}}) = \frac{\int_{E_{\text{cut}}} \frac{d\Gamma}{dE_L} dE_L}{\int_0 \frac{d\Gamma}{dE_L} dE_L} \quad (4)$$

can be used to extrapolate the measurement of the truncated branching fractions to zero cutoff:

$$BR_{c\ell\bar{\nu}} = \frac{\langle E_L^0 \rangle_{E_{\text{cut}}}}{R(E_{\text{cut}})} . \quad (5)$$

In addition to the *BABAR* measurement we also include the HFAG average at  $E_{\text{cut}} = 0.6$  GeV of  $(10.29 \pm 0.18)\%$  [28]. In order to utilize more than only one of these truncated branching fractions, one has to include the total branching fraction  $BR_{c\ell\bar{\nu}}$  as a free parameter in the fit. Together with the input of the averaged  $B$  meson lifetime  $\tau_B = 1.585 \pm 0.007$  ps this can be used to calculate the semileptonic width  $\Gamma_{SL}^{c\ell\bar{\nu}}$  as part of the  $\chi^2$  minimization. The HQE for  $\Gamma_{SL}^{c\ell\bar{\nu}}$  is directly related to  $|V_{cb}|^2$  (see Eq. 1) and introducing  $|V_{cb}|$  as a free parameter therefore has the advantage of determining the error on this quantity directly from the global fit. With this approach also potential non-Gaussian errors (*e.g.* asymmetric errors) of the fit parameters are properly propagated into the error on  $|V_{cb}|$ .

The fit to the moment measurements is carried out using the HQE calculations in the kinetic scheme presented in Refs. [2] and [4], including  $E_{\text{cut}}$  dependent perturbative corrections to the hadron moments [6, 29, 30]. However, rather than using linearized tables to determine  $\vec{M}_{\text{HQE}}$  (as was done previously in Ref. [7]), we obtain the prediction for every single moment from an analytical calculation [31]. This not only allows us to study the scale dependence of the kinetic scheme in detail but also provides more accurate predictions for the individual moments. Since some criticism has recently been raised concerning the quality of the theoretical expansion for the non-integer hadron moments  $\langle M_X \rangle$  and  $\langle M_X^3 \rangle$ , we exclude these moments from the fit until the issue of the theoretical uncertainty of these moment predictions is resolved. However, for comparison, we will always show their prediction based on the fit results and compare them with the corresponding measurements.

As  $\mu_G^2$  and  $\rho_{LS}^3$  are estimated from the  $B^* - B$  mass splitting and heavy-quark sum rules, respectively, we impose Gaussian error constraints of  $\mu_G^2 = 0.35 \pm 0.07$  GeV $^2$  and  $\rho_{LS}^3 = -0.15 \pm 0.10$  GeV $^3$  on these parameters as advocated in Ref. [2].

#### C. Theoretical Error Estimates

Since this analysis targets a measurement of the CKM matrix element  $|V_{cb}|$  with a relative error below the 2% level it

TABLE I: Summary of moment measurements used in the combined fit.  $n$  indicates the order of the (central) moment measurement of observable  $\langle M_X^n \rangle_{E_{\text{cut}}}$ ,  $\langle E_\ell^n \rangle_{E_{\text{cut}}}$  and  $\langle E_\gamma^n \rangle_{E_{\text{cut}}}$ .  $E_{\text{cut}}$  indicates measurements with the corresponding minimum lepton momenta and photon energies in GeV.

Experiment	Hadron Moments $\langle M_X^n \rangle_{E_{\text{cut}}}$	Lepton Moments $\langle E_\ell^n \rangle_{E_{\text{cut}}}$	Photon Moments $\langle E_\gamma^n \rangle_{E_{\text{cut}}}$
BABAR [14, 15] [16, 17]	$n=2$ $E_{\text{cut}}=0.9, 1.0, 1.1, 1.2, 1.3, 1.4, 1.5$ $n=4$ $E_{\text{cut}}=0.9, 1.0, 1.1, 1.2, 1.3, 1.4, 1.5$	$n=0$ $E_{\text{cut}}=0.6, 1.2, 1.5$ $n=1$ $E_{\text{cut}}=0.6, 0.8, 1.0, 1.2, 1.5$ $n=2$ $E_{\text{cut}}=0.6, 1.0, 1.5$ $n=3$ $E_{\text{cut}}=0.8, 1.2$	$n=1$ $E_{\text{cut}}=1.9, 2.0$ <sup>a</sup> $n=2$ $E_{\text{cut}}=1.9$ <sup>a</sup>
Belle [18, 19]			$n=1$ $E_{\text{cut}}=1.8, 1.9$ $n=2$ $E_{\text{cut}}=1.8, 2.0$
CDF [22]	$n=2$ $E_{\text{cut}}=0.7$ $n=4$ $E_{\text{cut}}=0.7$		
CLEO [23, 24]	$n=2$ $E_{\text{cut}}=1.0, 1.5$ $n=4$ $E_{\text{cut}}=1.0, 1.5$		$n=1$ $E_{\text{cut}}=2.0$
DELPHI [27]	$n=2$ $E_{\text{cut}}=0.0$ $n=4$ $E_{\text{cut}}=0.0$ $n=6$ $E_{\text{cut}}=0.0$	$n=1$ $E_{\text{cut}}=0.0$ $n=2$ $E_{\text{cut}}=0.0$ $n=3$ $E_{\text{cut}}=0.0$	
HFAG [28]		$n=0$ $E_{\text{cut}}=0.6$	

<sup>a</sup>A total of six photon moments from Refs. [16] and [17] are used.

is of vital importance to take theoretical uncertainties into account, as currently estimated. The HQEs for the moments have theoretical uncertainties due to certain limitations in the accuracy of the calculations and certain approximations. As Eq. 2 illustrates, the heavy quark parameters extracted from the simultaneous fit to the moments are used for a residual correction to  $|V_{cb}^0|$ . It is therefore important to include their theoretical uncertainties in the total covariance matrix of the  $\chi^2$  fit to achieve realistic error estimates for them and for  $|V_{cb}|$ .

Since the HQE for  $\Gamma_{SL}$  is the best known expansion in this framework also its error estimates are the most advanced. In Eq. 2 the HQE for  $|V_{cb}|$  is explicitly quoted with a theoretical uncertainty  $\delta_{th}$  to reflect the limited accuracy of this theoretical expression. Adding the individual uncertainties quoted in Ref. [3] in quadrature and accounting for the more advanced estimates of the potential importance of ‘intrinsic charm’ of Ref. [13], yields  $\delta_{th} = 1.4\%$ . We quote this error separately for  $|V_{cb}|$  and label it with a subscript ‘ $T_{SL}$ ’.

Following the recipe quoted in Ref. [2] we estimate the uncertainties in the individual HQEs for the moments  $M$  by conservatively varying the values of  $\mu_\pi^2$  and  $\mu_G^2$  by  $\pm 20\%$  and those of the  $O(1/m_b^3)$  operators  $\rho_{LS}^3$  and  $\rho_D^3$  by  $\pm 30\%$ . These variations are carried out around the expected theoretical values of  $\mu_\pi^2 = 0.4 \text{ GeV}^2$ ,  $\mu_G^2 = 0.35 \text{ GeV}^2$ ,  $\rho_D^3 = 0.2 \text{ GeV}^3$  and  $\rho_{LS}^3 = -0.15 \text{ GeV}^3$ . Perturbative uncertainties are addressed by varying  $\alpha_s$  by  $\pm 0.1$  for hadron moments and by  $\pm 0.04$  for lepton and photon moments around a central value of  $\alpha_s = 0.22$ . Finally, we also vary the quark masses  $m_b$  and  $m_c$  by 20 MeV around central values of 4.6 GeV and 1.18 GeV.

These uncertainties  $\sigma_{\xi_i}$  are propagated into an error on the individual moments  $\Delta M$  using Gaussian error propagation

$$(\Delta M)^2 = \sum_i \left( \frac{\partial M}{\partial \xi_i} \right)^2 \sigma_{\xi_i}^2 \quad (6)$$

where  $\xi = (m_b, m_c, \mu_\pi^2, \mu_G^2, \rho_D^3, \rho_{LS}^3, \alpha_s)$ . All these variations

are considered uncorrelated for a given moment. The theoretical covariance matrix is then constructed by treating these errors as fully correlated for a given moment with different  $E_{\text{cut}}$  while they are treated as uncorrelated between moments of different order.

For the moments of the photon energy spectrum we include additional theoretical errors related to the applied bias corrections as described in Ref. [4]. We follow the suggestion of the authors and take 30% of the absolute value of the particular bias as its uncertainty [32]. In addition we linearly add half the difference in the moments derived from the two distribution function ansätze as given in Ref. [4]. These additional theoretical errors related to the photon energy moments are considered to be uncorrelated for moments with different  $E_{\text{cut}}$  and of different order.

Generally, the chosen approach for the evaluation of the theoretical uncertainties is conservative. As a result of this the  $\chi^2/N_{\text{dof}}$  is very good as will be shown in the next section. It is interesting to note though, that a fit that neglects the theoretical errors leads to similar results. However, we consider the choice of theoretical errors as appropriate since we are trying to consistently extract  $|V_{cb}|$  and the heavy quark distribution function parameters from a fit to all moment measurements, and aim to arrive at a reliable error on  $|V_{ub}|$ . The conservative approach is also reflected in the fact that we exclude non-integer hadron moments and photon moments above  $E_{\text{cut}} = 2.0 \text{ GeV}$  from the fit.

#### D. Fit Results

In the following we present the results of a combined fit of the HQEs to all moment measurements listed in Table I along with their corresponding theoretical error estimates as defined in Section III C.

In order to assess the consistency of the moment measurements from the two different decay processes,  $B \rightarrow X_c \ell \bar{\nu}$  and  $B \rightarrow X_s \gamma$ , we also carry out separate fits to  $B \rightarrow X_c \ell \bar{\nu}$

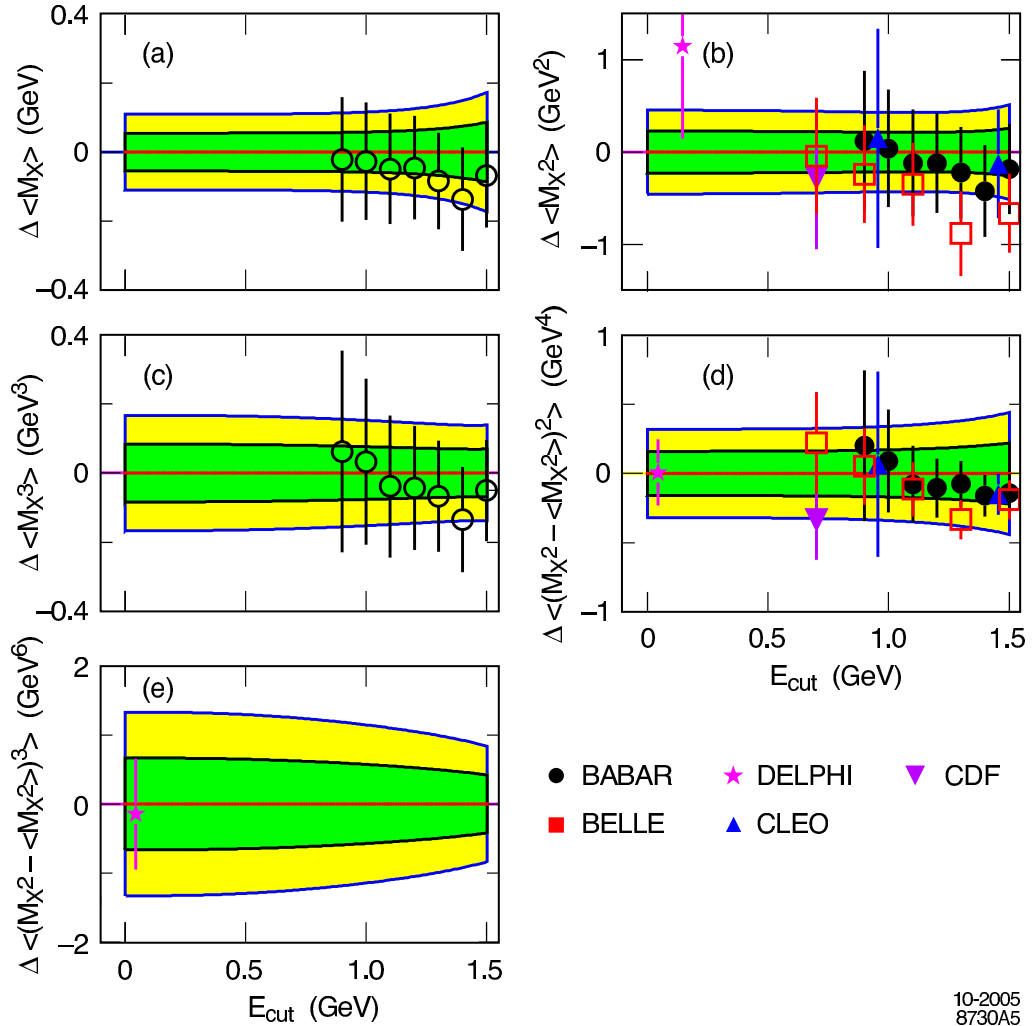


FIG. 1: *Difference* between the fit predictions and the hadron moment measurements: (a)  $\langle M_X \rangle$ , (b)  $\langle M_X^2 \rangle$ , (c)  $\langle M_X^3 \rangle$ , (d)  $\langle (M_X^2 - \langle M_X^2 \rangle)^2 \rangle$  and (e)  $\langle (M_X^2 - \langle M_X^2 \rangle)^3 \rangle$ . The yellow bands represent the total experimental and theoretical fit uncertainty as obtained by converting the fit errors of each individual HQE parameter into an error for the individual moment. The green band indicates the experimental uncertainty only. Solid markers are included in the fit while open markers are only overlaid for comparison. Moment measurements at different  $E_{cut}$  are highly correlated.

moments and to photon moments only. However, as the latter are not sensitive to all the heavy quark parameters, all but  $m_b$  and  $\mu_\pi^2$  are fixed to the result obtained from the combined fit.

A detailed comparison of the HQE predictions obtained from the combined fit and the moment measurements is shown in Figures 1-3 for the hadron, lepton and photon moments, respectively. The yellow bands represent the total experimental and theoretical fit uncertainty as obtained by converting the fit errors for each individual HQE parameter into an error for the individual moment. The green band indicates the experimental error only. These figures also show the measurements that are not included in the fit for the reasons described in Section III A. In particular the non-integer hadron moments  $\langle M_X \rangle$  and  $\langle M_X^3 \rangle$  can therefore be directly compared with the corresponding fit prediction. It can be seen that all moment measurements agree with each other and that the fit is able

to describe all the moment measurements of different order and from different  $B$  decay distributions.

Figure 3 shows a comparison of the fit prediction for the first and second moments of the photon energy spectrum for the standard OPE ansatz with the  $E_{cut}$  dependent bias corrected OPE calculations of Ref. [4]. While it is expected that the pure local OPE approach will break down at higher values of  $E_{cut}$  this is the first time that the accuracy of the experimental moment measurements is sufficient to demonstrate this effect. For  $E_{cut}$  above 2.0 GeV it is clearly visible that the pure OPE ansatz fails to describe the data.

The fit results are summarised in Table II where the separation of the errors into experimental and theoretical contributions was obtained from toy Monte Carlo experiments. The results are in good agreement with earlier determinations [7, 8, 9] but have improved accuracy. A comparison of results from the combined fit with those obtained from fits

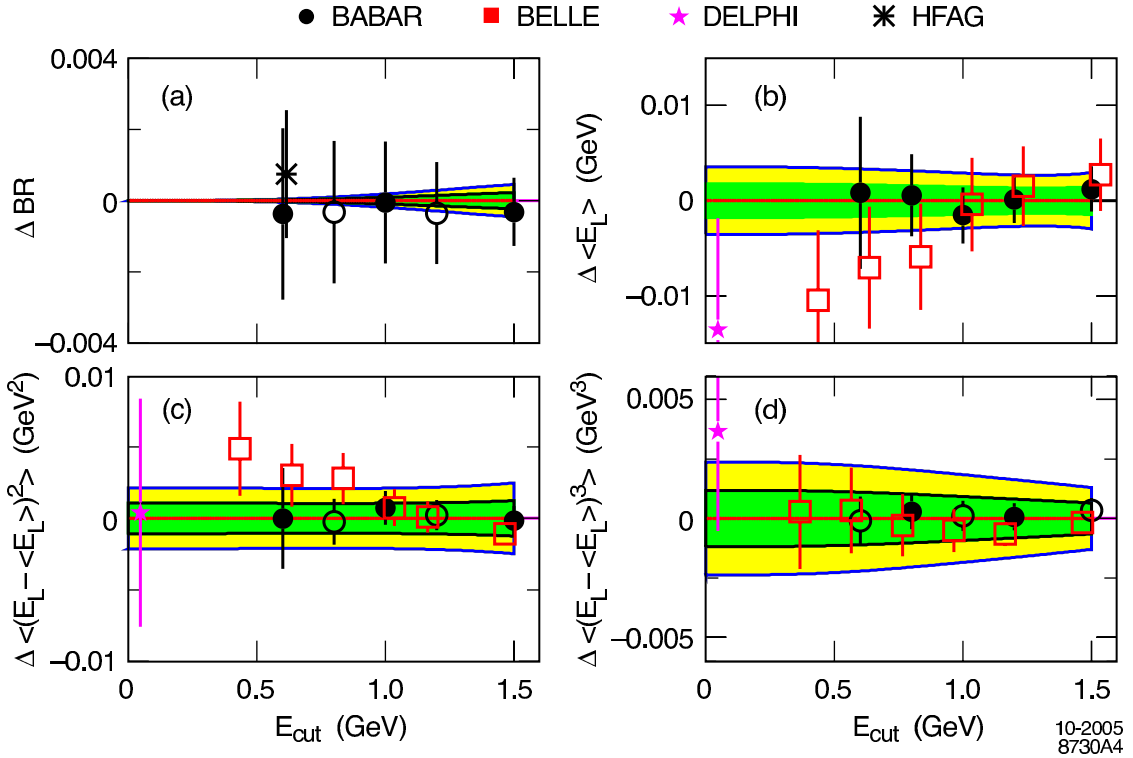


FIG. 2: Difference between the fit predictions and measurements for the lepton moments: (a)  $BR$ , (b)  $\langle E_L \rangle$ , (c)  $\langle (E_L - \langle E_L \rangle)^2 \rangle$  and (d)  $\langle (E_L - \langle E_L \rangle)^3 \rangle$ . The yellow bands represent the total experimental and theoretical fit uncertainty while the green band indicates the experimental uncertainty only. Solid markers are included in the fit while open markers are only overlaid for comparison. Moment measurements at different  $E_{cut}$  are highly correlated.

to  $B \rightarrow X_c \ell \bar{\nu}$  and  $B \rightarrow X_s \gamma$  moments only can be found in Figure 4 where the  $\Delta\chi^2 = 1$  contours for the fit results are shown in the  $(m_b, |V_{cb}|)$  and  $(m_b, \mu_\pi^2)$  planes. It can be seen that the inclusion of the photon energy moments adds additional sensitivity to the b-quark mass  $m_b$ .

Including the Belle measurements of the hadron mass and lepton energy moments with only their statistical correlations leads to very similar results with only small improvements in the errors for the heavy quark parameters. This is a consequence of the fit errors being dominated by the theoretical uncertainties as can be seen from Table II. For a future average based on the full covariance matrix it will be necessary to consider the strong correlation of the systematic errors of the lepton moments between experiments. In particular, a consistent background modeling and subtraction technique will be required.

To ensure the stability of the fit procedure several cross checks have been carried out. For instance, the combined fit has been repeated without applying the theoretical constraints on  $\mu_G^2$  and  $\rho_{LS}^3$ . We also repeated the fit excluding hadron moments with units  $\text{GeV}^6$  and lepton moments with units  $\text{GeV}^3$  as these moments are believed to have large theoretical uncertainties (as can be seen from Figures 1 and 2). In addition, photon moments with  $E_{cut} > 1.8 \text{ GeV}$  were excluded as here the bias corrections become noticeable. Finally a fit neglecting all theoretical errors was performed, i.e. only the experimental covariance matrix was used. All these results agree well with each other and any variations are fully covered by the theoretical error estimates. In addition

the scale dependence of the expressions for the moments was studied but was found to be small compared to the assigned theoretical uncertainties.

In addition to the above we extract the difference in the quark masses as

$$m_b - m_c = 3.446 \pm 0.025 \text{ GeV}.$$

Comparing the extracted values of the quark masses  $m_b$  and  $m_c$  with other determinations is often convenient in the commonly used  $\overline{\text{MS}}$  scheme. The translation between the kinetic and  $\overline{\text{MS}}$  masses to two loop accuracy and including the BLM part of the  $\alpha_s^3$  corrections was given in Ref. [3]. This leads to

$$\begin{aligned} \overline{m_b}(\overline{m_b}) &= 4.20 \pm 0.04 \text{ GeV} \\ \overline{m_c}(\overline{m_c}) &= 1.24 \pm 0.07 \text{ GeV} \end{aligned}$$

However, it has been accepted among theorists that the normalization scale of around 1.2 GeV in the  $\overline{\text{MS}}$  scheme may be too low for a precision evaluation of masses, and higher-order perturbative corrections in  $\overline{m_c}(\overline{m_c})$  are too significant. As a result, an additional uncertainty in  $\overline{m_c}(\overline{m_c})$  of at least 50 MeV may have to be added associated with the definition of  $\overline{m_c}(\overline{m_c})$  itself. A larger normalization scale for the  $\overline{\text{MS}}$  masses is generally used. To address this we give here the value of  $m_c$  normalized at a safer momentum scale 2.5 GeV as was advocated recently:

$$\overline{m_c}(2.5 \text{ GeV}) = 1.072 \pm 0.06 \text{ GeV}$$

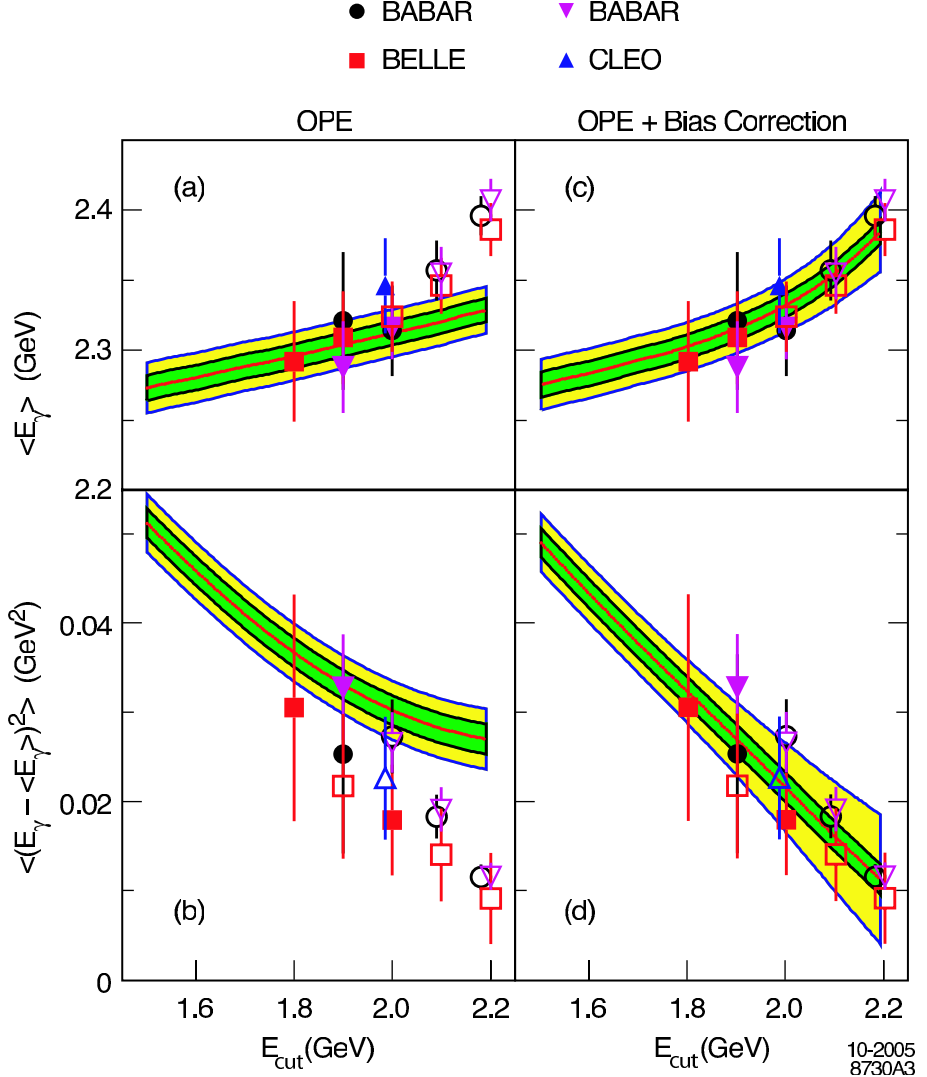


FIG. 3: Comparison of fit predictions and measurements for the photon moments: (a)  $\langle E_\gamma \rangle$  and (b)  $\langle (E_\gamma - \langle E_\gamma \rangle)^2 \rangle$ . The bands in the figures on the left show the fit prediction for the pure OPE calculation neglecting effects of the minimal photon energy cut on the OPE part (biases). The bands in figures (c) and (d) include those bias corrections of Ref. [4]. The yellow bands represent the total experimental and theoretical fit uncertainty while the green band indicates the experimental uncertainty only. Solid markers are included in the fit while open markers are only overlaid for comparison. Moment measurements at different  $E_{cut}$  are highly correlated.

the theoretical uncertainty in this translation is small. It may also be convenient to have the ratio of the charm and the beauty quark masses in the  $\overline{\text{MS}}$  scheme which is normalization-scale independent:

$$\frac{\overline{m}_c(\mu)}{\overline{m}_b(\mu)} = 0.235 \pm 0.012.$$

The uncertainty in this ratio is dominated by the fit error on  $m_c$ .

#### IV. TRANSLATION OF FIT RESULTS INTO OTHER SCHEMES

We translate the results for  $m_b$  and  $\mu_\pi^2$  in the kinetic scheme to heavy quark distribution function parameters in other schemes so that they can be used for the extraction of  $|V_{ub}|$ . The translation is done by predicting the first and second moment of the photon energy spectrum above  $E_{cut} = 1.6$  GeV based on the heavy quark parameters from Table II and using the calculations of Ref. [4].

The experimental and theoretical uncertainties in the fitted parameters as well as their correlations are propagated into the errors on the moments as described in Section III C. The minimum photon energy of 1.6 GeV is chosen such as to be insensitive to the distribution function itself. At this thresh-

TABLE II: Results for the combined fit to all moments with experimental and theoretical uncertainties. For  $|V_{cb}|$  we add an additional theoretical error stemming from the uncertainty in the expansion for  $\Gamma_{SL}$  of 1.4%. Below the fit results the correlation matrix is shown.

Combined Fit	OPE FIT RESULT: $\chi^2/N_{dof} = 19.3/44$							
	$ V_{cb}  \times 10^{-3}$	$m_b$ (GeV)	$m_c$ (GeV)	$\mu_\pi^2$ (GeV $^2$ )	$\rho_D^3$ (GeV $^3$ )	$\mu_G^2$ (GeV $^2$ )	$\rho_{LS}^3$ (GeV $^3$ )	$BR_{cl\nu}$ (%)
RESULT	41.96	4.590	1.142	0.401	0.174	0.297	-0.183	10.71
$\Delta_{\text{exp}}$	0.23	0.025	0.037	0.019	0.009	0.024	0.054	0.10
$\Delta_{\text{HQE}}$	0.35	0.030	0.045	0.035	0.022	0.046	0.071	0.08
$\Delta_{\Gamma_{SL}}$	0.59							
$ V_{cb} $	1.000	-0.399	-0.220	0.405	0.267	-0.305	0.056	0.700
$m_b$		1.000	0.951	-0.387	-0.189	0.074	-0.223	0.098
$m_c$			1.000	-0.408	-0.246	-0.329	-0.124	0.143
$\mu_\pi^2$				1.000	0.685	0.257	-0.008	0.122
$\rho_D^3$					1.000	-0.050	-0.479	-0.055
$\mu_G^2$						1.000	-0.035	0.046
$\rho_{LS}^3$							1.000	-0.052
$BR_{cl\nu}$								1.000

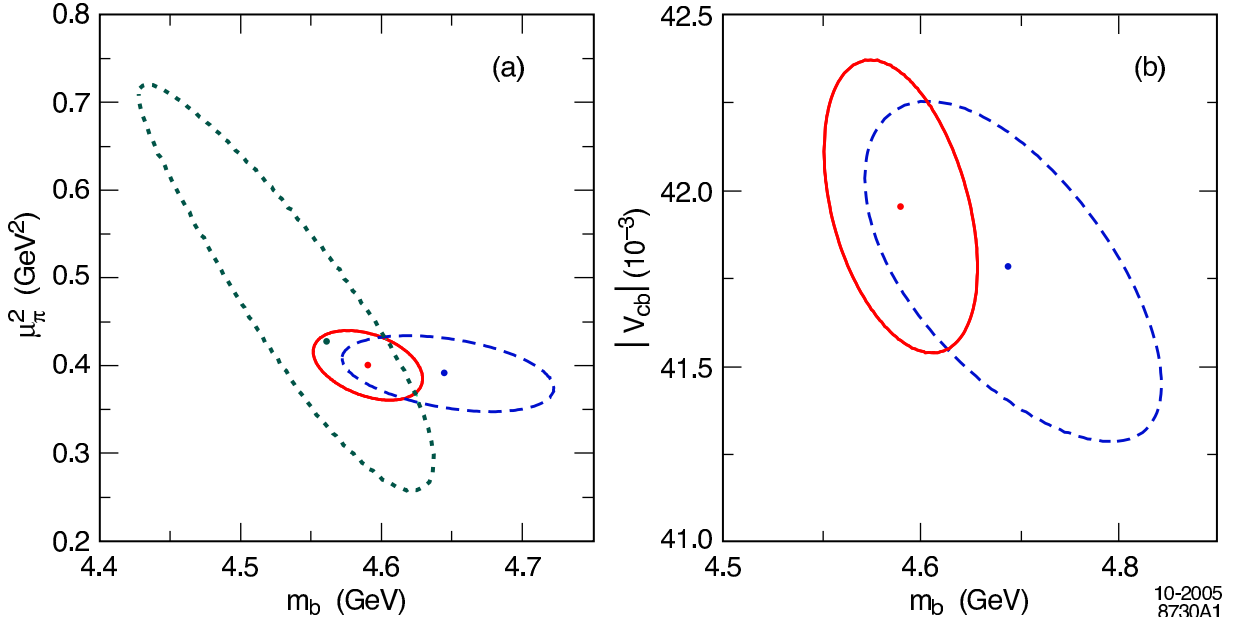


FIG. 4: Comparison of the different fit scenarios. Figure (a) shows the  $\Delta\chi^2 = 1$  contour in the  $(m_b, \mu_\pi^2)$  plane for the combined fit to all moments (solid red), the fit to hadron and lepton moments only (dashed blue) and the fit to photon moments only (dotted green). Figure (b) shows the results for the combined fit (solid red) and the fit to hadron and lepton moments only (dashed blue) in the  $(m_b, |V_{cb}|)$  plane.

old the local OPE calculation is applicable as the hardness  $Q = m_B - 2E_{\text{cut}}$  of the process is sufficiently high such that cut-induced perturbative and non-perturbative corrections or biases are negligible. The predicted moments are given in Table III.

As the moments are physical observables which are scheme independent they can be used to extract the corresponding heavy quark distribution function parameters in other schemes. For this translation, grids for the first and second moments of the photon energy spectrum are gener-

ated as a function of the two parameters  $(\bar{\Lambda}, \lambda_1)$  for Kagan-Neubert [33] and  $(m_b \text{ SF}, \mu_\pi^2 \text{ SF})$  for the Shape Function [34] scheme. A  $\chi^2$  is calculated for every set of parameters  $\mu = (\langle E_\gamma \rangle (m_b, \mu_\pi^2), \langle (E_\gamma - \langle E_\gamma \rangle)^2 \rangle (m_b, \mu_\pi^2))$  as

$$\chi^2 = \sum_{i,j=1,2} (y_i - \mu_i) V_{ij}^{-1} (y_j - \mu_j) \text{ with } V_{ij} = \sigma_i \sigma_j \rho_{ij} \quad (7)$$

where the  $y_i$  are the predicted moments with their errors  $\sigma_i$  and  $\rho_{ij}$  is the correlation between them.

From the minimum value  $\chi^2_{\min}$  we obtain the central values

TABLE III: First and second moment of the photon spectrum predicted for  $E_{\text{cut}} = 1.6$  GeV on the basis of the fit results for the HQE parameters.

$E_{\text{cut}}$ (GeV)	$\langle E_{\gamma} \rangle$ (GeV)	$\langle (E_{\gamma} - \langle E_{\gamma} \rangle)^2 \rangle$ (GeV $^2$ )	$\rho$
1.6	$2.284 \pm 0.018$	$0.0428 \pm 0.0032$	-0.03

TABLE IV: Comparison of heavy quark distribution function parameters in the kinetic, Kagan-Neubert and Shape Function scheme together with their correlation  $\rho$ .

Kinetic Scheme		
$m_b$ (GeV)	$\mu_{\pi}^2$ (GeV $^2$ )	$\rho$
$4.590 \pm 0.039$	$0.401 \pm 0.040$	-0.39
Kagan-Neubert Scheme		
$\bar{\Lambda}$ (GeV)	$\lambda_1$ (GeV $^2$ )	$\rho$
$0.621 \pm 0.041$	$-0.497^{+0.072}_{-0.086}$	-0.17
Shape Function Scheme		
$m_b$ SF (GeV)	$\mu_{\pi}^2$ SF (GeV $^2$ )	$\rho$
$4.604 \pm 0.038$	$0.189 \pm 0.038$	-0.23

for the parameters in the other schemes and determine the  $\Delta\chi^2 = 1$  contour with respect to  $\chi^2_{\text{min}}$ .

### A. Kagan-Neubert scheme

In order to derive shape function parameters from the predicted moments in the Kagan-Neubert scheme [33] a grid of moments was generated for varying values of  $\bar{\Lambda}$  and  $\lambda_1$ . This was obtained using the Kagan-Neubert  $B \rightarrow X_s\gamma$  generator with the exponential Shape Function ansatz as implemented in the Babar Monte Carlo generator (EvtGen [35]). The results of this translation are shown in Table IV and Figure 5.

### B. Shape-Function scheme

For the translation into the Shape-Function scheme [34, 36] we use a grid of moments obtained with a *Mathematica* notebook based on Ref. [37, 38, 39, 40] that was provided to us by the authors. In this calculation the moments are determined from a spectrum that is obtained by convoluting a shape function with a perturbative kernel with next-to-leading order accuracy, where we use the exponential form for the shape function given in Ref. [37]. This calculation is conceptually similar to the one for  $B \rightarrow X_u\ell\bar{\nu}$  decays also presented in Ref. [37] which at present is used for the extraction of  $|V_{ub}|$  by several experiments. It therefore allows for a consistent determination of the shape function parameters for both,  $B \rightarrow X_s\gamma$  and  $B \rightarrow X_u\ell\bar{\nu}$  decays. The numerical results for the shape function parameters are shown in Table IV and the  $\Delta\chi^2 = 1$  contours are displayed in Figure 5.

## V. APPLICATIONS FOR IMPROVED HEAVY QUARK PARAMETERS

### A. Improved OPE Expression for $|V_{ub}|$

The results in the kinetic scheme for  $m_b$ ,  $\mu_{\pi}^2$ ,  $\mu_G^2$  and  $\rho_D^3$  have been used to give an updated expression for the standard local OPE formula for  $|V_{ub}|$  of Ref. [32, 41]:

$$|V_{ub}| = 4.268 \cdot 10^{-3} \cdot \sqrt{\frac{BR(B \rightarrow X_u\ell\nu)}{0.002} \frac{1.61\text{ps}}{\tau_B}} \times (1 \pm 0.012_{\text{QCD}} \pm 0.022_{\text{HQE}}). \quad (8)$$

The error labeled ‘QCD’ includes perturbative uncertainties and those from weak annihilation. However, in contrast to Ref. [41] we also include explicitly the  $1/m_b^3$  contribution from the  $\rho_D^3$  term which results in an improved ‘QCD’ error. The ‘HQE’ related uncertainty stems from the errors on  $m_b$ ,  $\mu_{\pi}^2$ ,  $\mu_G^2$  and  $\rho_D^3$  and takes correlations between the parameters into account (see Table II).

### B. Extrapolation Factors for Measured $B \rightarrow X_s\gamma$ Branching Fraction

The measurement of the  $B \rightarrow X_s\gamma$  branching fraction is experimentally very challenging and has only been achieved for photon energies above  $E_{\text{cut}} = 1.8 - 2.0$  GeV. On the contrary, theoretical calculations predict the  $B \rightarrow X_s\gamma$  branching fraction at much lower values of  $E_{\text{cut}}$  in order to avoid any dependence on the heavy quark distribution function. It is therefore customary to extrapolate measured branching fractions down to a value of 1.6 GeV where they can be compared to the theoretical calculations [42, 43]. Based on the heavy quark distribution function parameters in Table IV and the corresponding spectra we calculated a consistent set of extrapolation factors

$$R(E_{\text{cut}}) = \frac{BR(B \rightarrow X_s\gamma)_{E_{\text{cut}}}}{BR(B \rightarrow X_s\gamma)_{1.6 \text{ GeV}}} \quad (9)$$

for the kinetic, Kagan-Neubert and Shape-Function scheme. The results are summarised in Table V and Figure 6. The error was determined as the largest deviation from the central value obtained from a scan around the ellipses in Figures 4 and 5, where positive and negative errors were of comparable size. The results have been averaged where the total error was determined by combining the largest error from the scan of the error ellipses with half the maximum difference between any two models in quadrature. Figure 6 also shows the spectra corresponding to the central values of Table IV or equivalently to the predicted photon energy moments of Table III in the three schemes.

## VI. CONCLUSION

We have performed a fit to moments measurements from  $B \rightarrow X_c\ell\bar{\nu}$  and  $B \rightarrow X_s\gamma$  decays using calculations in the kinetic scheme [2, 3, 4]. The fit uses all currently available moment measurements from the *BABAR*, *Belle*, *CDF*, *CLEO* and *DELPHI* experiments that are publicly available with their

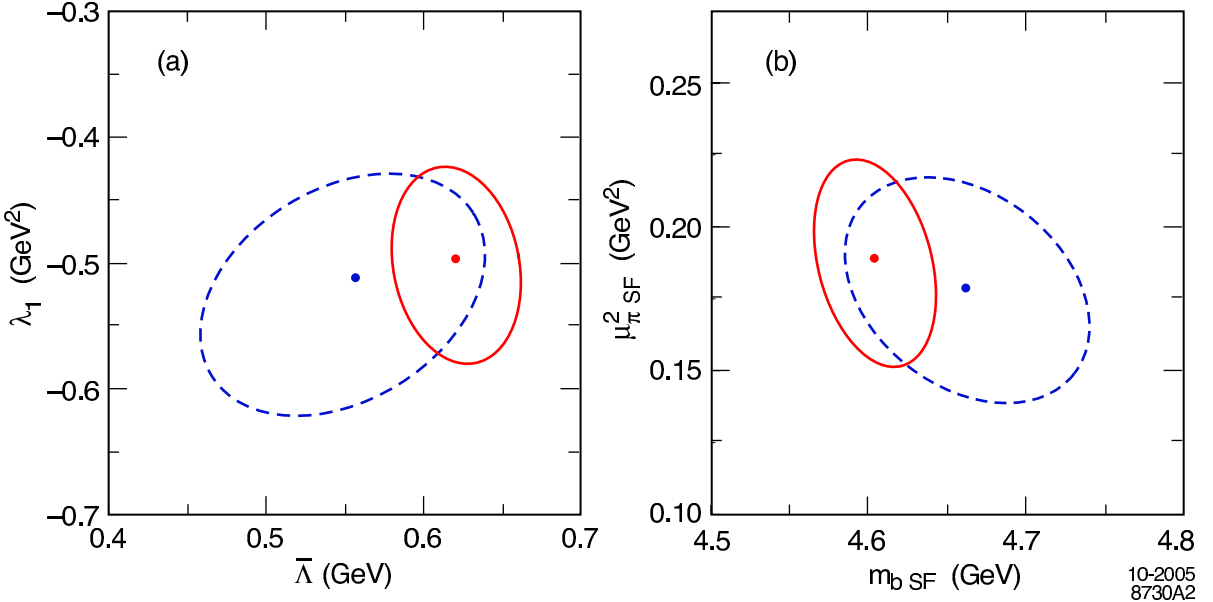


FIG. 5: Translation of fit results in the kinetic scheme to Kagan-Neubert (a) and the Shape Function scheme (b) via predicted photon moments. Figure (a) shows the results for the shape function parameters in the  $(\bar{\Lambda}, \lambda_1)$  plane from the combined fit to all moments (solid red) and the fit to hadron and lepton moments only (dashed blue). Figure (b) shows the corresponding fit results in the  $(m_b \text{ SF}, \mu_\pi^2 \text{ SF})$  plane.

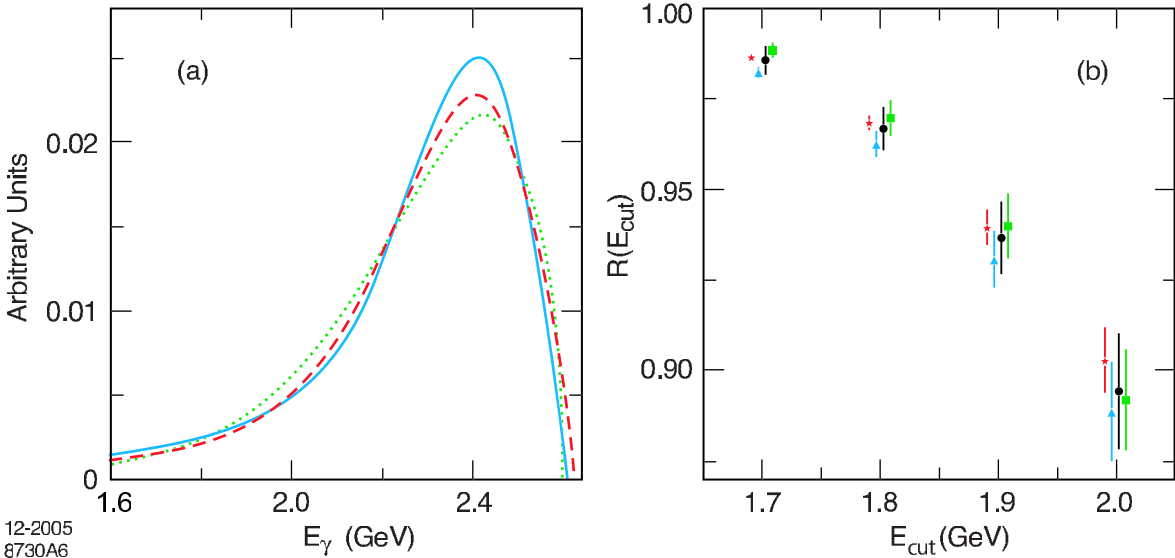


FIG. 6: Figure (a) shows the photon energy spectra corresponding to the fitted heavy quark distribution parameters in the kinetic scheme (dashed red), Shape Function scheme (solid blue) and Kagan-Neubert scheme (dotted green). Figure (b) shows the corresponding extrapolation factors  $R(E_{\text{cut}})$  for varying  $E_{\text{cut}}$  for the kinetic scheme (red stars), Shape Function scheme (blue triangles) and Kagan-Neubert scheme (green squares) together with our average (black circles).

corresponding correlation matrices. We find that all the moment measurements of different order and from different inclusive  $B$  decays can be described by the fit result which is an important test of the consistency of this theoretical framework. We have extracted values for the CKM matrix element  $|V_{cb}|$ , the quark masses  $m_b$  and  $m_c$ , and the kinetic expecta-

tion value  $\mu_\pi^2$  of

$$\begin{aligned}
 |V_{cb}| &= (41.96 \pm 0.23_{\text{exp}} \pm 0.35_{\text{HQE}} \pm 0.59_{\Gamma_{SL}}) \times 10^{-3} \\
 m_b &= 4.590 \pm 0.025_{\text{exp}} \pm 0.030_{\text{HQE}} \text{ GeV} \\
 m_c &= 1.142 \pm 0.037_{\text{exp}} \pm 0.045_{\text{HQE}} \text{ GeV} \\
 \mu_\pi^2 &= 0.401 \pm 0.019_{\text{exp}} \pm 0.035_{\text{HQE}} \text{ GeV}^2
 \end{aligned}$$

TABLE V: Extrapolation factors  $R(E_{\text{cut}})$  for  $\text{BR}(B \rightarrow X_s \gamma)$ .

$E_{\text{cut}}$ (GeV)	Kinetic Scheme	Kagan-Neubert Scheme	Shape Function Scheme	Average
1.7	$0.986 \pm 0.001$	$0.988 \pm 0.002$	$0.982 \pm 0.002$	$0.985 \pm 0.004$
1.8	$0.968 \pm 0.002$	$0.970 \pm 0.005$	$0.962 \pm 0.004$	$0.967 \pm 0.006$
1.9	$0.939 \pm 0.005$	$0.940 \pm 0.009$	$0.930 \pm 0.008$	$0.936 \pm 0.010$
2.0	$0.903 \pm 0.009$	$0.892 \pm 0.014$	$0.888 \pm 0.014$	$0.894 \pm 0.016$

where the first error includes statistical and systematic experimental uncertainties and the second the theoretical uncertainties from the HQEs.

As can be seen, the error on  $|V_{cb}|$  which is below 2% is dominated by theoretical uncertainties. Any further improvements will require additional work on the accuracy for the expression of  $\Gamma_{SL}$ , in particular on perturbative corrections to the Wilson coefficients of the chromomagnetic and Darwin operators. Similar observations can be made for  $m_b$ , which is determined with an accuracy of below 1%. However, the extraction of these quantities at the percent level represents in itself a remarkable test and success of the QCD-based calculations.

The values for  $m_b$  and  $\mu_\pi^2$  have been translated into the Kagan-Neubert Scheme where we obtain following values for the Shape Function parameters:

$$\begin{aligned}\bar{\Lambda} &= 0.621 \pm 0.041 \text{ GeV} \\ \lambda_1 &= -0.497^{+0.072}_{-0.086} \text{ GeV}^2\end{aligned}.$$

Similarly, we obtain

$$\begin{aligned}m_b \text{ SF} &= 4.604 \pm 0.038 \text{ GeV} \\ \mu_\pi^2 \text{ SF} &= 0.189 \pm 0.038 \text{ GeV}^2\end{aligned}$$

in the Shape Function scheme. As these parameters are critical for the extraction of  $|V_{ub}|$ , their reduced uncertainty will enable measurements of  $|V_{ub}|$  at the 5% level. This, together with  $|V_{cb}|$ , will provide for a competitive measurement of the side of the Unitarity Triangle opposite the angle  $\beta$ , and give further insights into the extent of CP violation in tree processes.

## VII. ACKNOWLEDGEMENTS

This work has greatly benefited from many interactions and exchanges with N. Uraltsev, P. Gambino and I. Bigi concerning the calculations in the kinetic scheme. The authors would also like to thank M. Neubert for many discussions regarding the calculations for  $B \rightarrow X_s \gamma$  decays in the shape function scheme. Furthermore, we would like to thank our colleagues of the *BABAR* Collaboration, in particular F. di Lodovico and V. Lüth, and our colleagues from HFAG for their valuable input to this analysis. H. F. is supported by a PPARC Postdoctoral Fellowship.

---

[1] A. F. Falk and M. E. Luke, Phys. Rev. **D57**, 424 (1998), hep-ph/9708327.

[2] P. Gambino and N. Uraltsev, Eur. Phys. J. **C34**, 181 (2004), hep-ph/0401063.

[3] D. Benson, I. I. Bigi, T. Mannel, and N. Uraltsev, Nucl. Phys. **B665**, 367 (2003), hep-ph/0302262.

[4] D. Benson, I. I. Bigi, and N. Uraltsev, Nucl. Phys. **B710**, 371 (2005), hep-ph/0410080.

[5] C. W. Bauer, Z. Ligeti, M. Luke, and A. V. Manohar, Phys. Rev. **D67**, 054012 (2003), hep-ph/0210027.

[6] N. Uraltsev, Int. J. Mod. Phys. **A20**, 2099 (2005), hep-ph/0403166.

[7] B. Aubert et al. (*BABAR* Collaboration), Phys. Rev. Lett. **93**, 011803 (2004), hep-ex/0404017.

[8] C. W. Bauer, Z. Ligeti, M. Luke, A. V. Manohar, and M. Trott, Phys. Rev. **D70**, 094017 (2004), hep-ph/0408002.

[9] M. Battaglia et al., Phys. Lett. **B556**, 41 (2003), hep-ph/0210319.

[10] I. I. Y. Bigi, M. A. Shifman, N. Uraltsev, and A. I. Vainshtein, Phys. Rev. **D56**, 4017 (1997), hep-ph/9704245.

[11] K. Melnikov and A. Mitov, Phys. Lett. **B620**, 69 (2005), hep-ph/0505097.

[12] S. Eidelman et al. (Particle Data Group), Phys. Lett. **B592**, 1 (2004), and 2005 partial update for edition 2006.

[13] I. I. Bigi, N. Uraltsev, and R. Zwicky (2005), hep-ph/0511158.

[14] B. Aubert et al. (*BABAR* Collaboration), Phys. Rev. **D69**, 111103 (2004), hep-ex/0403031.

[15] B. Aubert et al. (*BABAR* Collaboration), Phys. Rev. **D69**, 111104 (2004), hep-ex/0403030.

[16] B. Aubert et al. (*BABAR* Collaboration), Phys. Rev. **D72**, 052004 (2005), hep-ex/0508004.

[17] B. Aubert et al. (*BABAR* Collaboration), (2005), hep-ex/0507001.

[18] P. Koppenburg et al. (*Belle* Collaboration), Phys. Rev. Lett. **93**, 061803 (2004), hep-ex/0403004.

[19] K. Abe et al. (*Belle* Collaboration), (2005), hep-ex/0508005.

[20] K. Abe et al. (*Belle* Collaboration) (2005), hep-ex/0509013.

[21] K. Abe et al. (*Belle* Collaboration) (2005), hep-ex/0508056.

[22] D. Acosta et al. (*CDF* Collaboration), Phys. Rev. **D71**,

051103 (2005), hep-ex/0502003.

[23] S. E. Csorna et al. (CLEO Collaboration), Phys. Rev. **D70**, 032002 (2004), hep-ex/0403052.

[24] S. Chen et al. (CLEO Collaboration), Phys. Rev. Lett. **87**, 251807 (2001), hep-ex/0108032.

[25] A. H. Mahmood et al. (CLEO Collaboration), Phys. Rev. **D70**, 032003 (2004), hep-ex/0403053.

[26] A covariance matrix of the lepton energy moments can be found in: C. J. Stepaniak, Ph. D. thesis, University of Minnesota, (2004).

[27] J. Abdallah et al. (DELPHI), Eur. Phys. J. **C45**, 35 (2006), hep-ex/0510024.

[28] J. Alexander et al. (Heavy Flavor Averaging Group (HFAG)) (2005), hep-ex/0412073.

[29] M. Trott, Phys. Rev. **D70**, 073003 (2004), hep-ph/0402120.

[30] V. Aquila, P. Gambino, G. Ridolfi, and N. Uraltsev, Nucl. Phys. **B719**, 77 (2005), hep-ph/0503083.

[31] P. Gambino (2005), private communication.

[32] N. Uraltsev (2005), private communication.

[33] A. L. Kagan and M. Neubert, Eur. Phys. J. **C7**, 5 (1999), hep-ph/9805303.

[34] S. W. Bosch, B. O. Lange, M. Neubert, and G. Paz, Nucl. Phys. **B699**, 335 (2004), hep-ph/0402094.

[35] D. J. Lange, Nucl. Instrum. Meth. **A462**, 152 (2001).

[36] M. Neubert, Phys. Lett. **B612**, 13 (2005), hep-ph/0412241.

[37] B. O. Lange, M. Neubert, and G. Paz, Phys. Rev. **D72**, 073006 (2005), hep-ph/0504071.

[38] M. Neubert, Eur. Phys. J. **C44**, 205 (2005), hep-ph/0411027.

[39] S. W. Bosch, M. Neubert, and G. Paz, JHEP **11**, 073 (2004), hep-ph/0409115.

[40] M. Neubert, Eur. Phys. J. **C40**, 165 (2005), hep-ph/0408179.

[41] N. Uraltsev, Int. J. Mod. Phys. **A14**, 4641 (1999), hep-ph/9905520.

[42] P. Gambino and M. Misiak, Nucl. Phys. **B611**, 338 (2001), hep-ph/0104034.

[43] A. J. Buras, A. Czarnecki, M. Misiak, and J. Urban, Nucl. Phys. **B631**, 219 (2002), hep-ph/0203135.